Supplementary Materials for

Targeting clinical epigenetic reprogramming for chemoprevention of metabolic and viral hepatocellular carcinoma

Frank Jühling[1,2]†, Nourdine Hamdane[1,2]†, Emilie Crouchet[1,2]†, Shen Li[3]†, Houssein El Saghire[1,2], Atish Mukherji[1,2], Naoto Fujiwara[4], Marine A. Oudot[1,2], Christine Thumann[1,2], Antonio Saviano[1,2,5], Armando Andres Roca Suarez[1,2], Kaku Goto[1,2], Ricard Masia[6], Mozhdeh Sojoodi[3], Gunisha Arora[3], Hiroshi Aikata[7], Atsushi Ono[4,7], Parissa Tabrizian[8], Myron Schwartz[8], Stephen J. Polyak[9,10], Irwin Davidson[11], Christian Schmidl[12,13], Christoph Bock[12,14], Catherine Schuster[1,2], Kazuaki Chayama[7], Patrick Pessaux[1,2,5], Kenneth K. Tanabe[3], Yujin Hoshida[4], Mirjam B. Zeisel[1,2,15], François H.T. Duong[1,2], Bryan C. Fuchs[3#], Thomas F. Baumert[1,2,5,16#*]

†, # these authors contributed equally

*Correspondence to: Prof. Thomas F. Baumert, MD, Inserm U1110, University of Strasbourg, 3 Rue Koeberlé, F-67000 Strasbourg. Phone: +33368853703, email: thomas.baumert@unistra.fr

This PDF file includes:

- Legends of Supplementary Figures (S1-S8)
- Supplementary figures
- Legends of Supplementary Tables (S1-S7)
- Supplementary tables
- Supplementary Material and Methods

Jühling F, *et al. Gut* 2020;0:1–13. doi: 10.1136/gutjnl-2019-318918

Legends of Supplementary Figures:

Fig. S1 (related to figure 1A). Sequencing tag density of H3K27ac enrichment in the *NFκB2* gene in liver tissue of control, NASH, CHC and DAA-cured patients with HCC. H3K27ac ChIPmentation-based ChIP-Seq was performed on non-infected (Control 1-6; green), on NASH (NASH 1-7; brown), on CHC (CHC 1-6; red) and on DAA/HCC cured (DAA/HCC 1-6; orange) patient livers shown in Figure 1A. Blue boxes indicate called H3K27ac-enriched *loci*. Integrative Genomics Viewer (IGV) was used to illustrate reads on the *NFκB2* gene.

Fig. S2 (related to figure 2). NASH, CHC and DAA/HCC cured patients with advanced liver disease share epigenetic and transcriptional changes associated with HCC risk. (A) RNA-Seq (left panel) and ChIP-Seq (right panel) mapping of transcriptomic and H3K27ac modifications among NASH-, CHC- and DAA/HCC cured patient-derived liver biopsies and resections. Left panel: Unsupervised clustering of significant 5,786 differentially expressed genes in livers from NASH (n=**3**), CHC (n=**6**) and DAA/HCC cured (n=**3**) patients compared to control patients (n=3, 5 and 3 respectively). Right panel: Differential signals in H3K27ac ChIP-Seq peaks for corresponding genes in livers from NASH (n=**7**), CHC (n=**6**) and DAA/HCC cured (n=**6**) compared to control patients (n=6). (B) Significant H3K27ac modifications correlate (Spearman's rank correlation coefficients and p-values) with gene expression changes in DAA/HCC cured patients. Prognostic association of hepatic gene expression was determined as described for Fig. 1B. (C) Venn diagram showing the overlap of significant epigenetically modified genes with corresponding expression changes in NASH, CHC and DAA/HCC cured patients derived from the ChIP-Seq and RNA-Seq experiments shown in panel A. (D) H3K27ac changes of the 1,256 genes with significant transcriptomic changes in NASH, CHC and DAA/HCC cured patients derived from Fig. S2B. (E) H3K27ac

Jühling F, *et al. Gut* 2020;0:1–13. doi: 10.1136/gutjnl-2019-318918

modifications correlate (Spearman's rank correlation coefficients and p-values) with transcriptomic changes of gene members of the PLS in DAA/HCC cured patients. Prognostic association of hepatic gene expression was determined as described for Fig. 1B.

Fig. S3 (related to figure 3). Persistent HCV infection and FFA treatment led to shared epigenetic and transcriptomic changes (A) H3K27ac ChIPmentation-based ChIP-Seq was performed on non-infected Huh7.5.1^{dif} cells (Control 1-2; green), on HCV-infected cells (HCV 1-2; red), on non-treated coculture system (Mock 1-3; green) and on FFA-treated coculture (FFA 1-3; brown) as shown in Figure 3. Blue boxes indicate peak-called H3K27ac-enriched *loci*. Integrative Genomics Viewer (IGV) was used to illustrate reads on the *NFκB2* gene. (B) H3K27ac modifications correlate (Spearman's rank correlation coefficients and p-values) with transcriptomic changes of gene members of the PLS in FFA-treated cells (left panel) or HCV-infected cells (right panel) shown in Fig. 3C. Prognostic association of gene expression was determined using Cox score for time to overall death in a cohort of patients as described in the material and methods. (C) Gene expression and H3K27ac changes of the gene members of the PLS in FFA-treated cells correlates with changes observed in HCV-infected cells (Spearman's rank correlation coefficients and p-values).

Fig. S4 (related to figure 4G). Full length immunoblots. Protein analysis was performed in total cell lysates using a reducing 12% SDS-PAGE gel electrophoresis. Analysis of c-Myc, Actin and total proteins ("Stain-free") was performed on the same PVDF membrane. The marker size (Precision Plus Protein Standards All Blue, BioRad) are indicated for each membrane. Contrasts of western blotting images were equally adjusted for entire membranes using Bio-Rad image analysis software. Quantification of c-Myc expression was performed

Jühling F, *et al. Gut* 2020;0:1–13. doi: 10.1136/gutjnl-2019-318918

using Image Lab software (Biorad) and normalised to total protein amount (Stain-free technology).

Fig. S5 (related to supplementary Table S7). Venn diagram summarizing the table S7 and showing epigenetically and transcriptionally altered genes in CHC/NASH patients and in DEN/CDAHFD mice, that were corrected by JQ1 treatment. Genes that harbor epigenetic and transcriptomic changes were identified in CHC/NASH patients and in DEN/CDAHFD mice. Among the changed genes, we analyzed whether JQ1 could revert back their H3K27ac levels and their transcript expression levels.

Fig. S6 (related to figure 5H). Full length immunoblots from Figure 5H. Protein analysis was performed on proteins extracted from mouse liver tissues, using a reducing 12% SDS-PAGE gel electrophoresis. Analysis of c-Myc, Actin and total proteins ("Stain-free") was performed on the same PVDF membrane. The marker size (Precision Plus Protein Standards All Blue, BioRad) are indicated for each membrane. Contrasts of western blotting images were equally adjusted for entire membranes using Bio-Rad image analysis software. Quantification of c-Myc expression was performed using Image Lab software (Biorad) and normalised to total protein amount (Stain-free technology).

Fig. S7 (related to figure 5). JQ1 treatment of HCV-infected Huh7.5.1^{dif} cells and DEN/CDAHFD mice does not alter YAP protein expression. Analysis of protein level of YAP and phospho-YAP proteins (pYAP Ser127, inactivated form of YAP protein) in (A) Mock and HCV-infected Huh7.5.1^{dif} cells treated or not with JQ1 and in (B) the livers of control (PBS), vehicle, and JQ1-treated CDAHFD-DEN mice by Western blot analyses. For each membrane, « Stain-free » corresponds to the total protein levels.

Fig. S8 (related to figure 6). The therapeutic effect of JQ1 is independent of chromatin reader expression. (A) Expression of BRD3, BRD4, HDAC9, KMT2A/MLL, and WRD5 in healthy donors and NASH patients from 2 public repositories. (B) KMT2A/MLL expression is associated to HCC risk in an CHC-HCC cohort. (C) Expression of BRD3, BRD4, HDAC9, KMT2A/MLL, and WRD5 in healthy donors, CHC patients and NASH patients from the patient cohort described in this study. Results are expressed in percentage of normalised read counts for the different RNA-seq experiments performed within this study. ** = $p < 0.01$ (D) Expression of the chromatin reader in DEN/CDAHFD mice treated with vehicle control or JQ1. Results are expressed in percentage of normalised read counts from RNA-seq experiments.

Jühling F, *et al. Gut* 2020;0:1–13. doi: 10.1136/gutjnl-2019-318918

Supplementary figures

Fig. S1

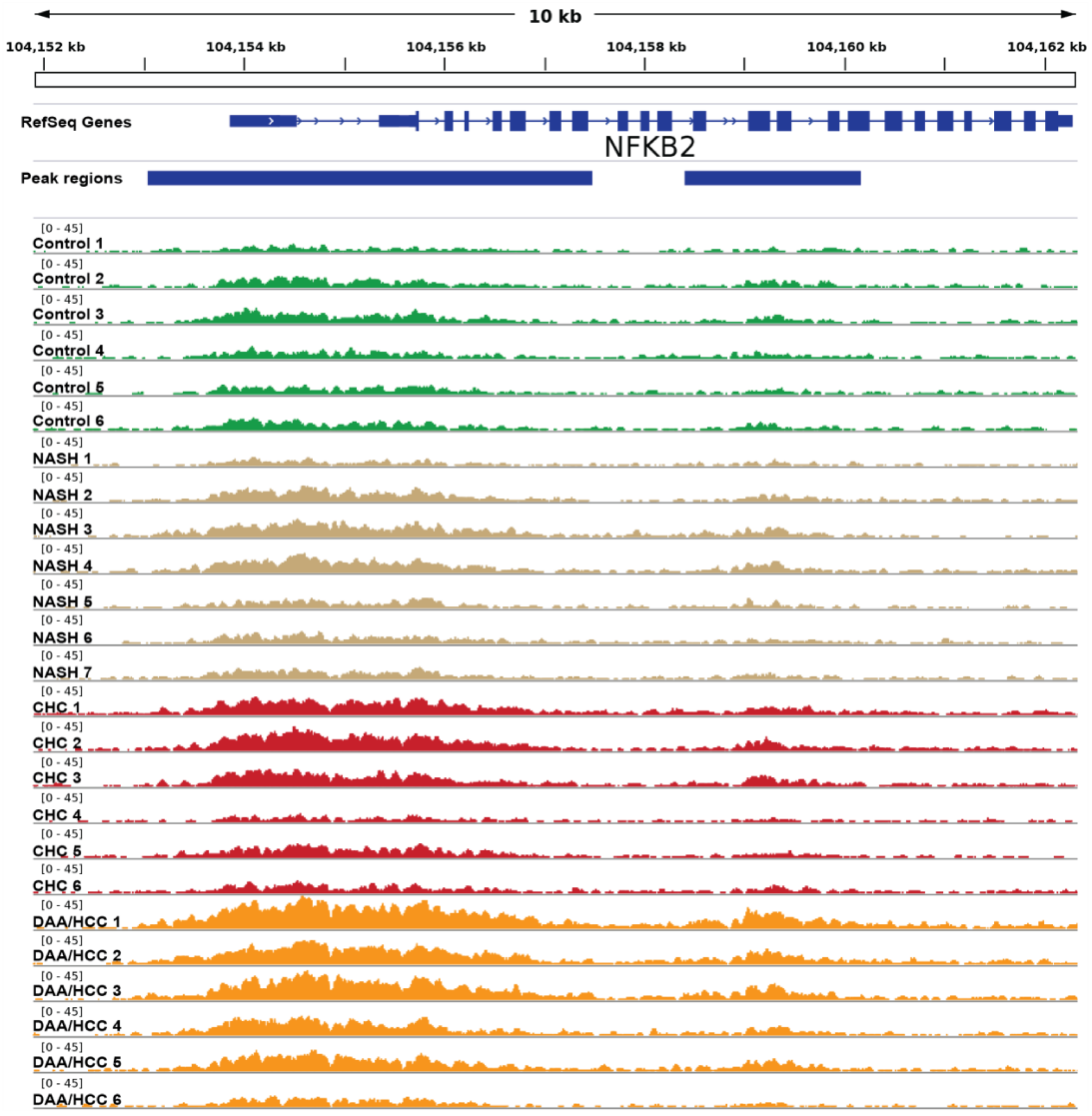

Fig. S2

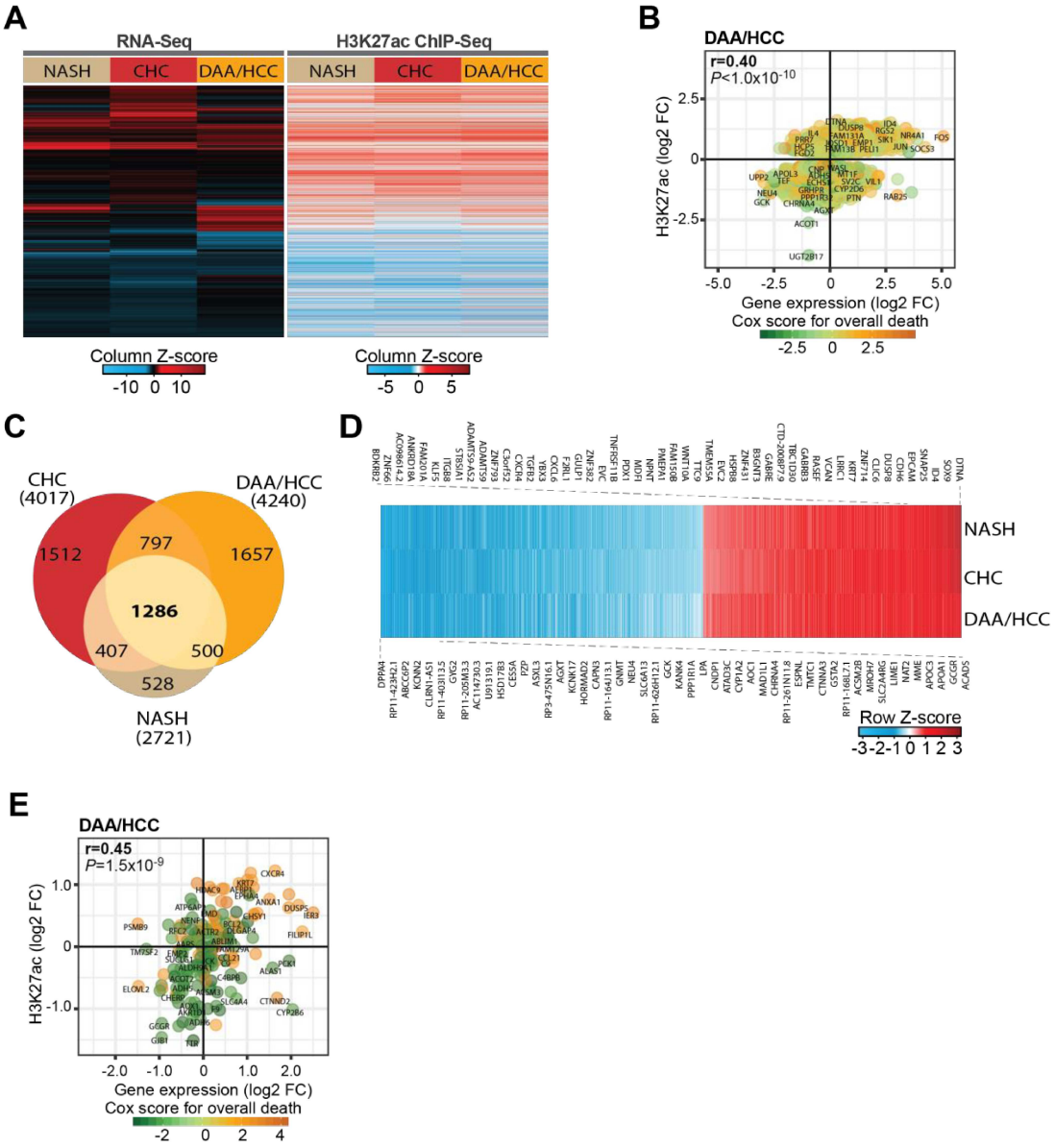
A
RNA-Seq
H3K27ac ChIP-Seq
NASH
CHC
DAA/HCC
Column Z-score
-10 0 10
-5 0 5
B
DAA/HCC
r=0.40
P<1.0x10-10
H3K27ac (log2 FC)
Gene expression (log2 FC)
Cox score for overall death
C
CHC (4017)
DAA/HCC (4240)
NASH (2721)
1512
797
1657
1286
407
500
528
D
NASH
CHC
DAA/HCC
Row Z-score
E
DAA/HCC
r=0.45
P=1.5x10-9
H3K27ac (log2 FC)
Gene expression (log2 FC)
Cox score for overall death

Fig. S3

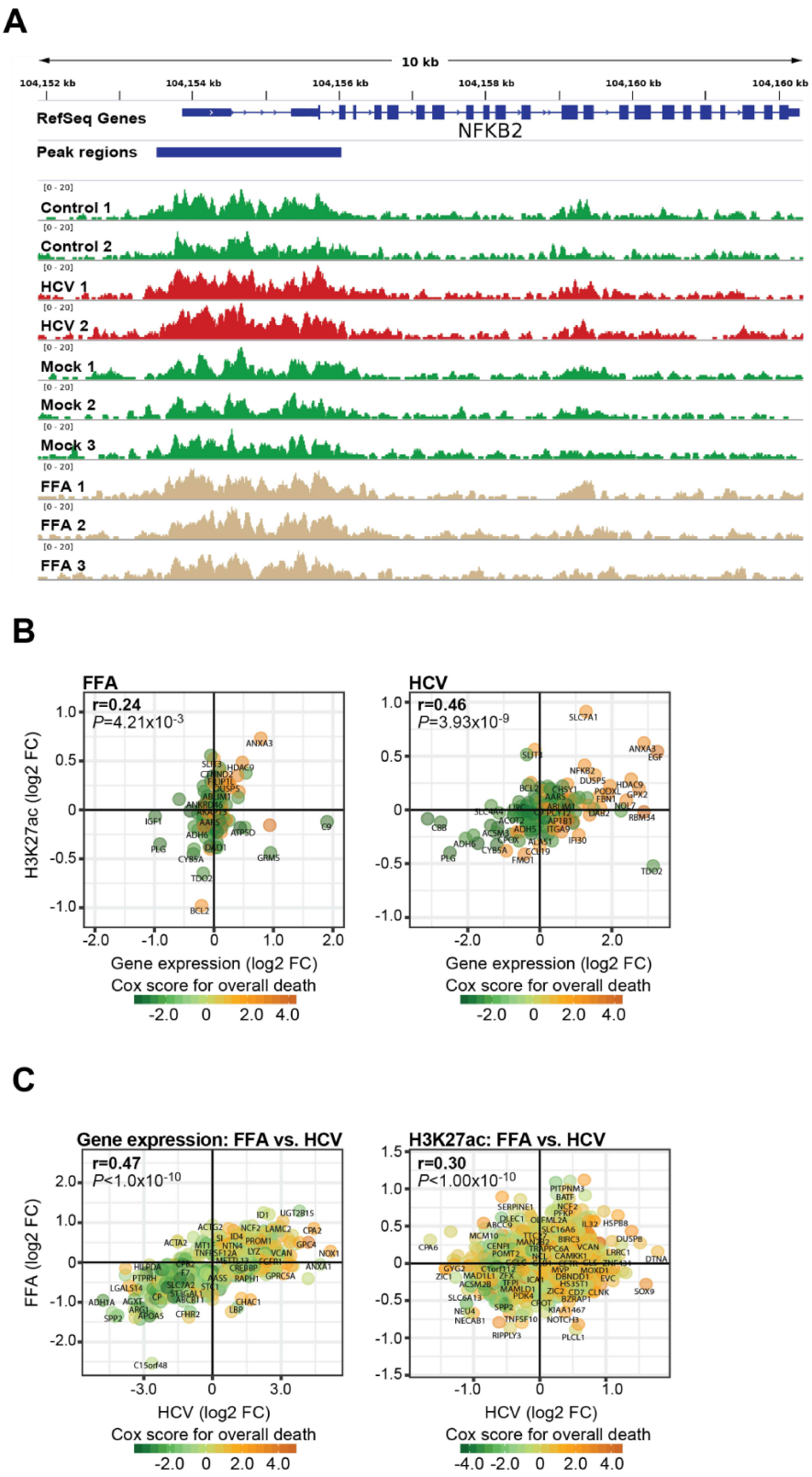
A
10 kb
104,152 kb
104,154 kb
104,156 kb
104,158 kb
104,160 kb
104,160 kb
RefSeq Genes
NFKB2
Peak regions
Control 1
Control 2
HCV 1
HCV 2
Mock 1
Mock 2
Mock 3
FFA 1
FFA 2
FFA 3
B
FFA
r=0.24
P=4.21x10-3
HCV
r=0.46
P=3.93x10-9
H3K27ac (log2 FC)
Gene expression (log2 FC)
Cox score for overall death
C
Gene expression: FFA vs. HCV
r=0.47
P<1.0x10-10
H3K27ac: FFA vs. HCV
r=0.30
P<1.00x10-10
FFA (log2 FC)
HCV (log2 FC)
Cox score for overall death

Fig. S4

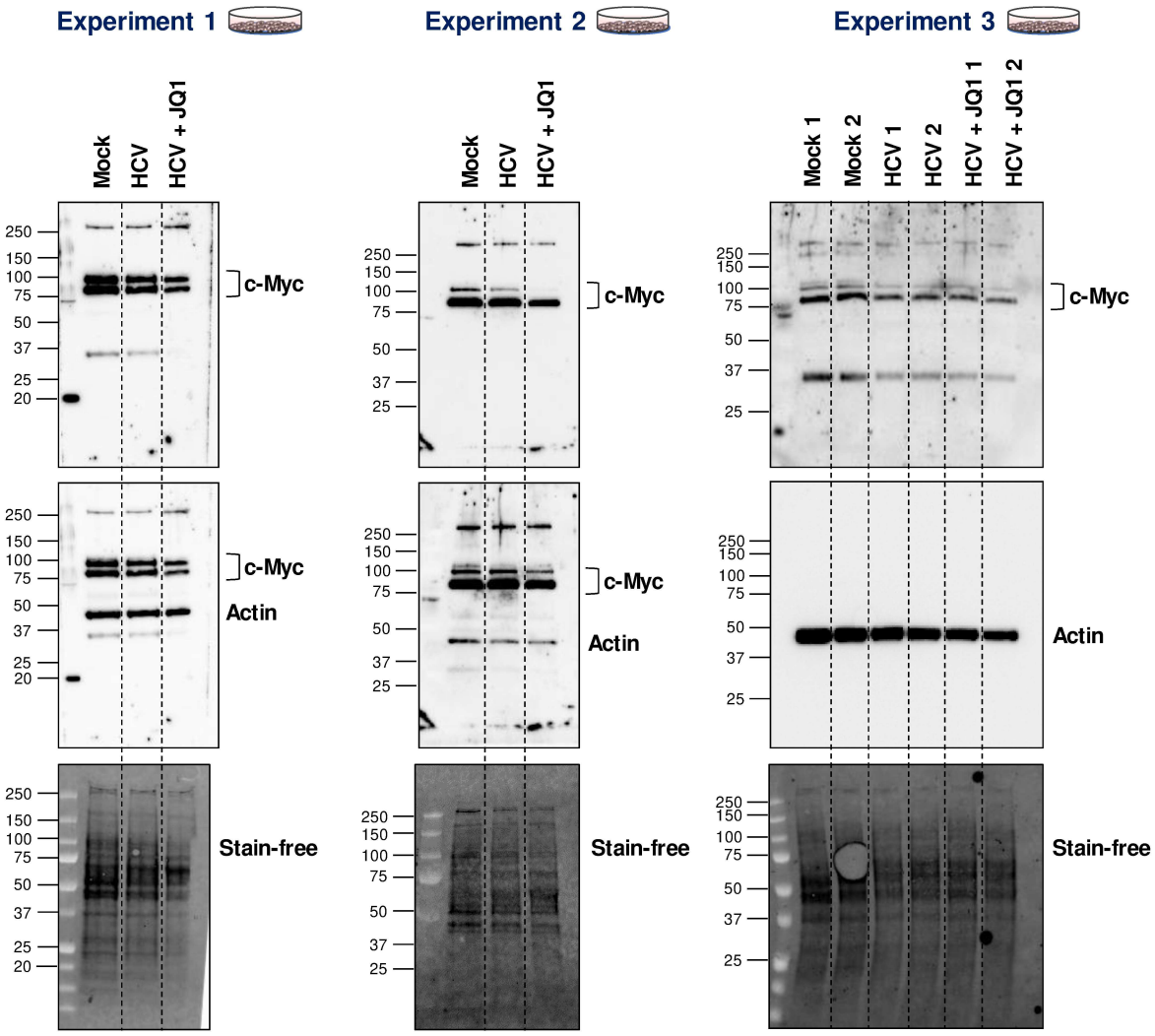

Jühling F, *et al. Gut* 2020;0:1–13. doi: 10.1136/gutjnl-2019-318918

Fig. S5

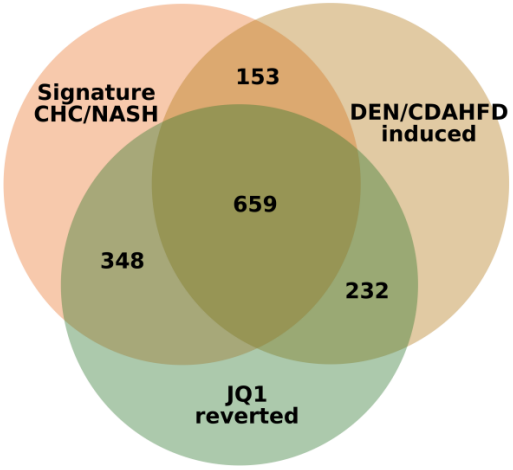

Jühling F, *et al. Gut* 2020;0:1–13. doi: 10.1136/gutjnl-2019-318918

Fig. S6

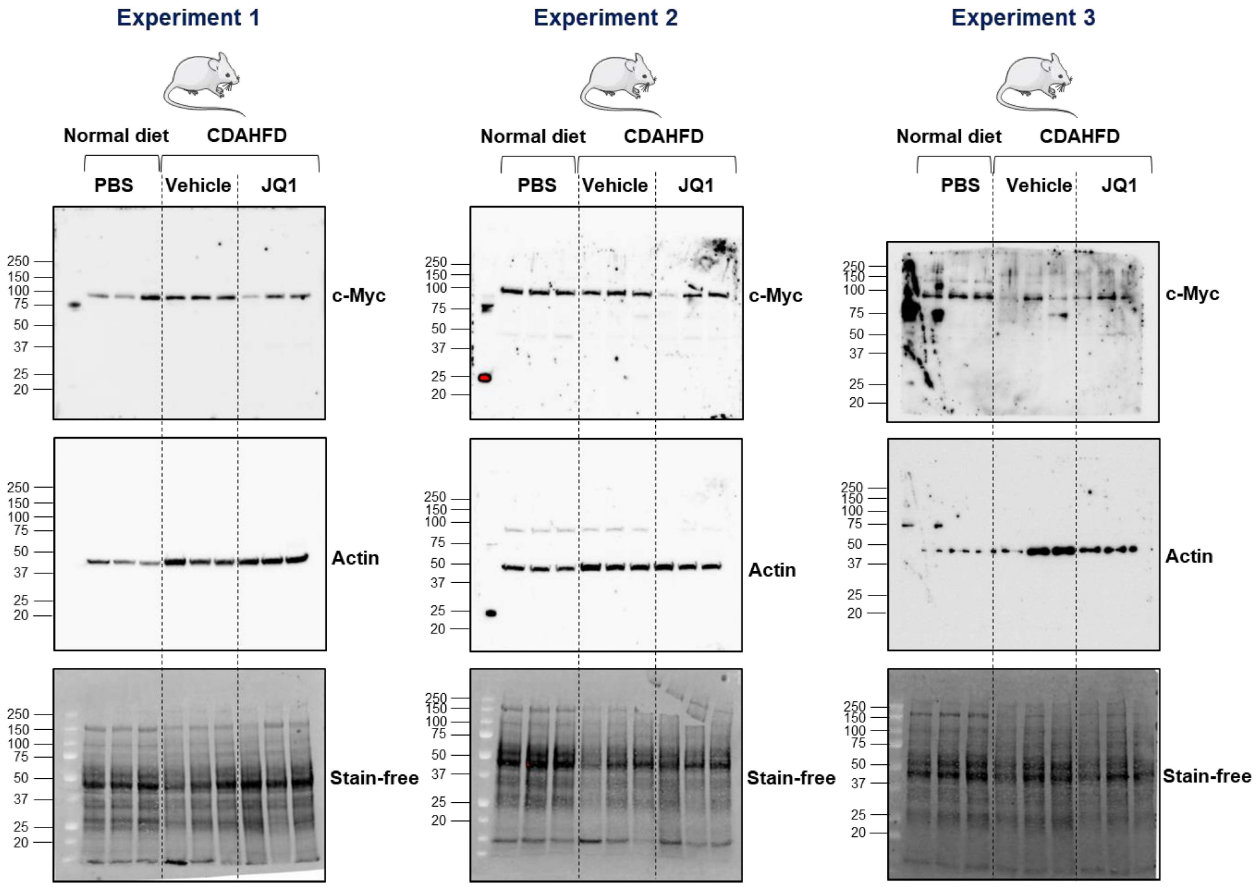
Experiment 1
Experiment 2
Experiment 3
Normal diet
CDAHFD
PBS
Vehicle
JQ1
c-Myc
Actin
Stain-free
250
150
100
75
50
37
25
20

Fig. S7

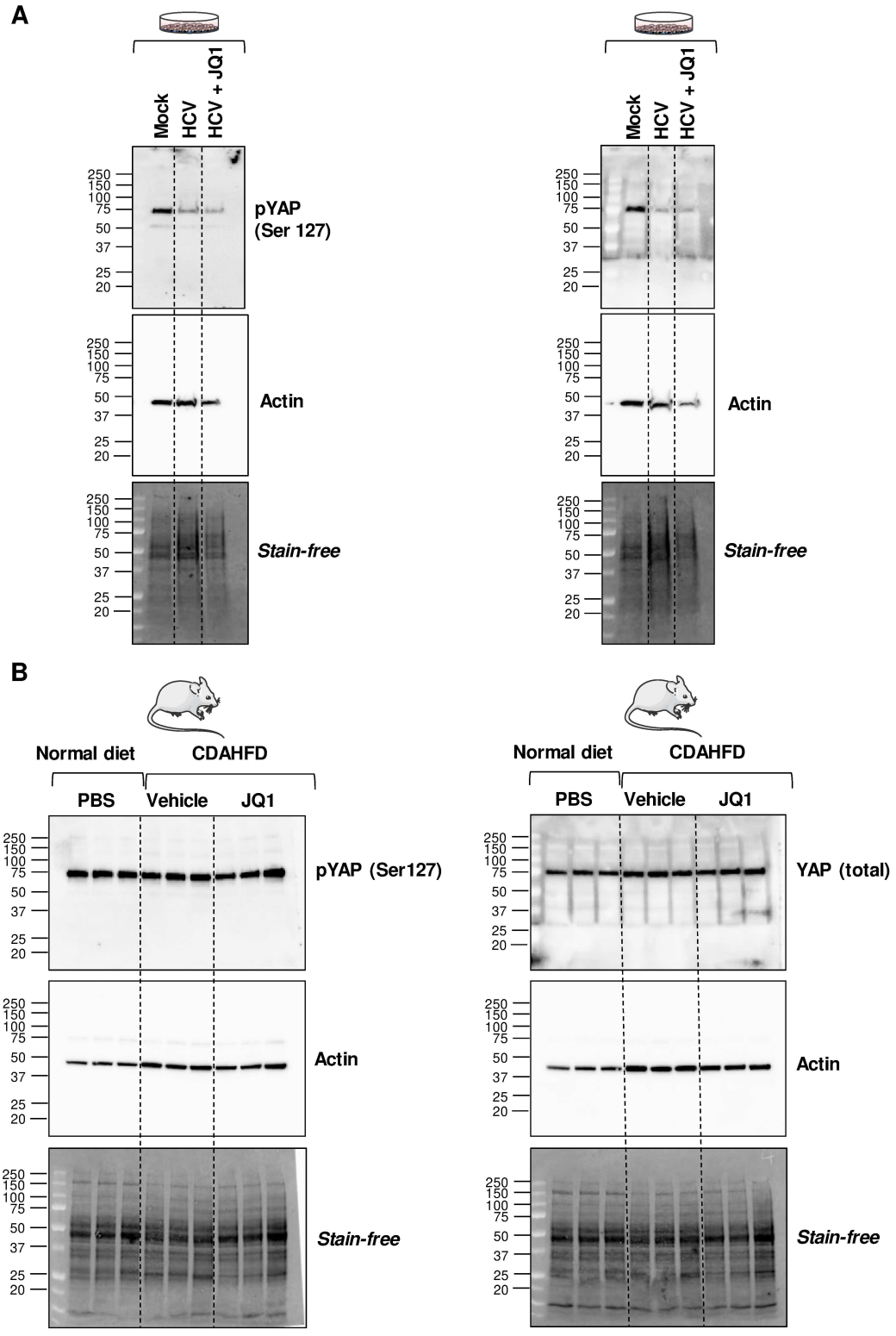
A
Mock
HCV
HCV + JQ1
pYAP (Ser 127)
Actin
Stain-free
Mock
HCV
HCV + JQ1
Actin
Stain-free
B
Normal diet
CDAHFD
PBS
Vehicle
JQ1
pYAP (Ser127)
Actin
Stain-free
Normal diet
CDAHFD
PBS
Vehicle
JQ1
YAP (total)
Actin
Stain-free

Fig. S8

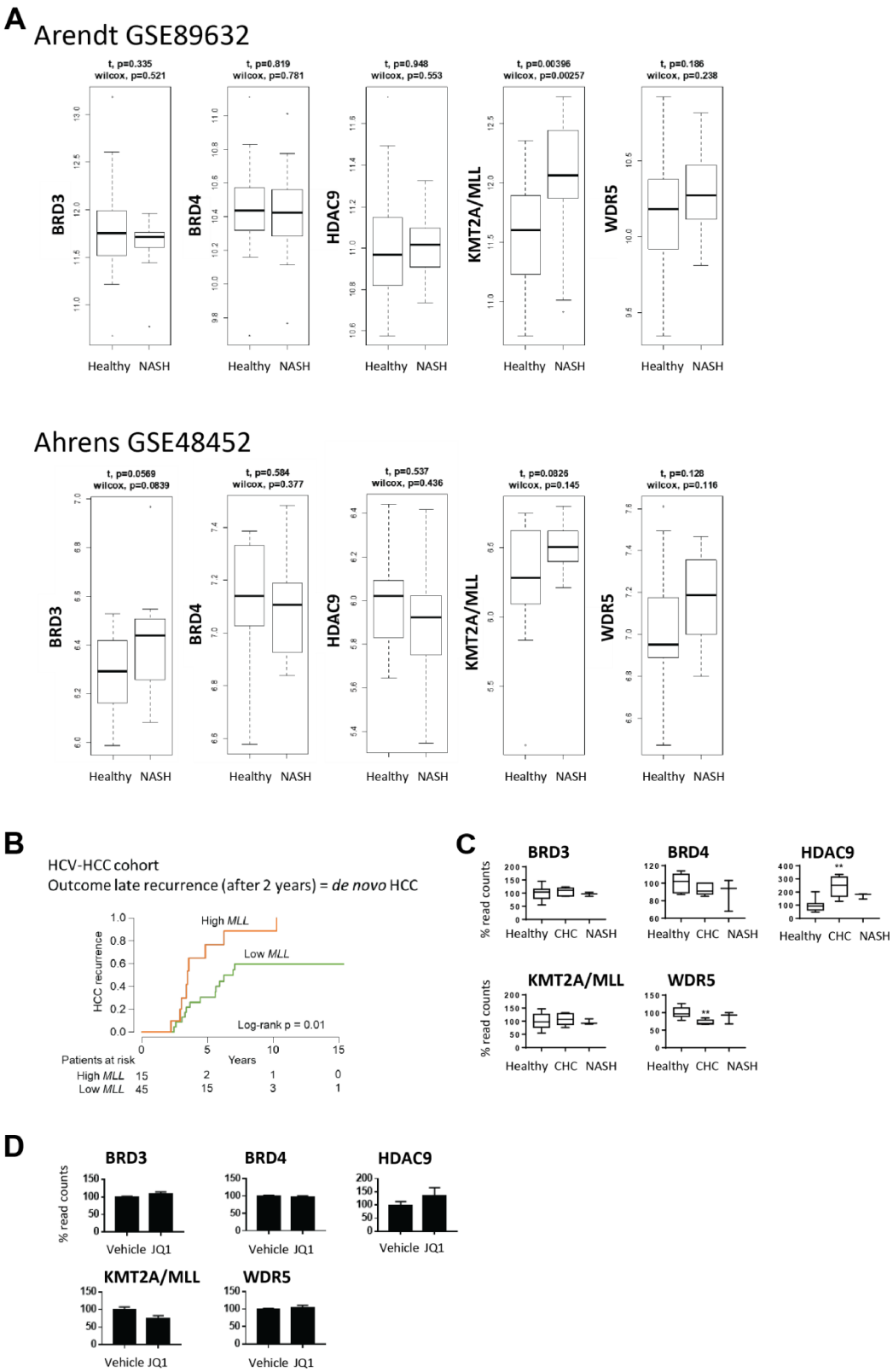
A
Arendt GSE89632
t, p=0.335
wilcox, p=0.521
t, p=0.819
wilcox, p=0.781
t, p=0.948
wilcox, p=0.553
t, p=0.00396
wilcox, p=0.00257
t, p=0.186
wilcox, p=0.238
BRD3
BRD4
HDAC9
KMT2A/MLL
WDR5
Healthy NASH
Ahrens GSE48452
t, p=0.0569
wilcox, p=0.0839
t, p=0.584
wilcox, p=0.377
t, p=0.537
wilcox, p=0.436
t, p=0.0826
wilcox, p=0.145
t, p=0.128
wilcox, p=0.116
B
HCV-HCC cohort
Outcome late recurrence (after 2 years) = *de novo* HCC
HCC recurrence
High *MLL*
Low *MLL*
Log-rank p = 0.01
Years
Patients at risk
High *MLL* 15 2 1 0
Low *MLL* 45 15 3 1
C
BRD3
BRD4
HDAC9
KMT2A/MLL
WDR5
% read counts
Healthy CHC NASH
D
BRD3
BRD4
HDAC9
KMT2A/MLL
WDR5
% read counts
Vehicle JQ1

Legends of Supplementary Tables:

Table S1. Clinical data of patients included in epigenetic analyses using ChIP-seq (related to Fig. 1). Fibrosis was staged according to Kleiner score[1] for NASH and METAVIR score[2] for all the other etiologies. METAVIR score was used for histological grading of the activity of HCV infection[3]. ASV= asunaprevir, CHC= chronic hepatitis C, DCV= daclatasvir, HCC = hepatocellular carcinoma, HCV= hepatitis C virus, LDV= ledipasvir, N/A=not applicable, NASH= non-alcoholic steatohepatitis, RBV= ribavirin, SOF= sofosbuvir.

Table S2. Clinical data of patients included in the spheroid experiments (related to Fig. 6). Fibrosis was staged according to Kleiner score[1] for NASH and METAVIR score[2] for all the other etiologies. METAVIR score was used for histological grading of the activity of HCV infection[3]. CHC = chronic hepatitis C, HCA = hepatocellular adenoma, HCC = hepatocellular carcinoma, NAFLD = non-alcoholic fatty liver disease, NASH = non-alcoholic steatohepatitis, PEG IFN = pegylated interferon, RBV = ribavirin

Table S3 (related to figure 1D). Epigenetic (H3K27ac) log2FCs of 1,693 common genes in NASH and CHC patients with similar significant epigenetic modifications and corresponding transcriptional changes.

Table S4 (related to Fig. 2C). List of the 25 genes of the prognostic epigenetic signature (PES). List of the 25 genes (high and low-risk genes) with the highest prediction of HCC risk

Jühling F, *et al. Gut* 2020;0:1–13. doi: 10.1136/gutjnl-2019-318918

predicted from the 1,693 commonly changed genes on CHC and NASH patients (FDR<0.25) shown in Fig. 2C. The dysregulation was determined by the nearest template prediction[4].

Table S5 (related to figure S2C). Epigenetic (H3K27ac) log2FCs of 1,286 common genes in NASH, CHC, and DAA-cured patients with similar significant epigenetic modifications and corresponding transcriptional changes.

Table S6 (related to figure 3B). Epigenetic (H3K27ac) log2FCs of 244 common genes in NASH and CHC patients, and HCV-infected Huh7.5.1^{dif} cells with similar significant epigenetic modifications and corresponding transcriptional changes.

Table S7 (related to figure 5B). Transcriptional changes of the 1,693 common genes in NASH and CHC patients that show similar significant epigenetic modifications and corresponding transcriptional changes and of vehicle and JQ1-treated DEN/CDAHFD mice.

Jühling F, *et al. Gut* 2020;0:1–13. doi: 10.1136/gutjnl-2019-318918

Table S1

Group	Gender	Age	Liver disease	Tumor	Viral genotype	METAVIR grade	Fibrosis stage	Antiviral treatment	Viral load (log10 IU/ml)
Controls	F	55	Minimal hepatitis	No	N/A	N/A	F0	N/A	N/A
Controls	M	46	Minimal hepatitis	No	N/A	N/A	F0	N/A	N/A
Controls	F	40	Lobular hepatitis	No	N/A	N/A	F0	N/A	N/A
Controls	F	53	Minimal hepatitis	No	N/A	N/A	F0	N/A	N/A
Controls	M	56	Lobular hepatitis	No	N/A	N/A	F0	N/A	N/A
Controls	F	58	Minimal hepatits	No	N/A	N/A	F0	N/A	N/A
HCC w/o liver disease	F	71	No	HCC	N/A	N/A	F0	N/A	N/A
HCC w/o liver disease	M	66	No	HCC	N/A	N/A	F0	N/A	N/A
HCC w/o liver disease	F	65	No	HCC	N/A	N/A	F0	N/A	N/A
NASH	M	65	NASH	HCC	N/A	N/A	F1	N/A	N/A
NASH	M	84	NASH	HCC	N/A	N/A	F1	N/A	N/A
NASH	M	78	NASH	HCC	N/A	N/A	F1	N/A	N/A
NASH	M	27	NASH	No	N/A	N/A	F4	N/A	N/A
NASH	M	63	NASH	HCC	N/A	N/A	F4	N/A	N/A
NASH	M	73	NASH	HCC	N/A	N/A	F4	N/A	N/A
NASH	M	76	NASH	HCC	N/A	N/A	F4	N/A	N/A
NASH	F	65	NASH	No	N/A	N/A	F4	N/A	N/A
NASH	F	47	NASH	No	N/A	N/A	F4	N/A	N/A
NASH	F	68	NASH	No	N/A	N/A	F4	N/A	N/A
CHC	M	52	CHC	No	1a	A3	F3	Naïve	5.82
CHC	M	54	CHC	HCC	1b	A1	F4	Relapse to SOF/DCV/RBV	4.64
CHC	M	68	CHC	HCC	2a	A3	F3	Naïve	5.40
CHC	F	48	CHC	No	3a	A3	F4	Naïve	6.06
CHC	M	65	CHC	No	1b	A2	F4	Naïve	6.35
CHC	M	51	CHC	HCC	3a	A2	F4	Relapse to SOF/RBV	6.58
Cured CHC	M	58	Cured CHC	HCC	1a	A0	F4	SOF/LDV	Undetectable
Cured CHC	F	79	Cured CHC	HCC	1b	A2	F4	DCV/ASV	Undetectable
Cured CHC	M	63	Cured CHC	HCC	2a	A2	F4	SOF/RBV	Undetectable
Cured CHC	M	69	Cured CHC	HCC	1b	A2	F3	DCV/ASV	Undetectable
Cured CHC	M	73	Cured CHC	HCC	1b	A2	F3	DCV/ASV	Undetectable
Cured CHC	M	75	Cured CHC	HCC	1b	A2	F3	SOF/LDV	Undetectable

ASV = asunaprevir, CHC = chronic hepatitis C, DCV = daclatasvir, HCC = hepatocellular carcinoma, HCV = hepatitis C virus, LDV= ledipasvir, N/A=not applicable, NASH = non-alcoholic steatohepatitis, RBV = ribavirin, SOF = sofosbuvir

Table S2

Group	Gender	Age	Liver disease	Tumor	Viral genotype	METAVIR Grade	Fibrosis Stage	Antiviral treatment	Viral load (log10 UI/ml)
Spheroids	M	72	NASH	HCC	N/A	N/A	F4	N/A	N/A
Spheroids	M	83	No	HCC	N/A	N/A	F1	N/A	N/A
Spheroids	M	72	NASH	HCC	N/A	N/A	F4	N/A	N/A
Spheroids	M	65	Cured CHC	HCC	3	A1	F1	PEG IFN and RBV	Undetectable
Spheroids	F	28	NAFLD	HCA	N/A	N/A	F0	N/A	N/A

CHC = chronic hepatitis C, HCA = hepatocellular adenoma, HCC = hepatocellular carcinoma, NAFL= non-alcoholic fatty liver, NASH= non-alcoholic steatohepatitis, PEG IFN = pegylated interferon, RBV=ribavirin

Jühling F, *et al. Gut* 2020;0:1–13. doi: 10.1136/gutjnl-2019-318918

Table S4

High risk genes
GPRIN3
COL1A2
SLC7A6
CHST11
LBH
TRPC1
IGF2BP2
ARRDC2
SELM
TMED3

Low risk genes
GSTA1
GRB14
SERPINA5
CAT
SLC25A1
PKLR
ADH4
GLYAT
TTR
HPX
RARRES2
ACADSB
CFHR5
DCXR
GALK1

Jühling F, *et al. Gut* 2020;0:1–13. doi: 10.1136/gutjnl-2019-318918

Supplementary material and methods:

Reagents and antibodies. DMSO, WDR5-0103, SAHA, JQ1 and Thapsigargin were purchased from Sigma-Aldrich, C646, CTK7A and MM-102 from Merck Millipore, I-BET151 from Tocris Bioscience, TSA from Selleckchem, TMP150 from Cellagen, HCV core-specific antibody (#MA1-080) and BAPTA from ThermoFisher, H3K27ac (#39134), BRD3 (#61489), BRD4 (#39909) and HDAC9 (#61401) antibodies from Active Motif, c-Myc antibody from Genetex (#GTX103436) and Actin (#ab8226) antibody from Abcam, rabbit anti-YAP1 (#4912) and anti-YAP-S127 (D9W2I; #13008) antibodies from Cell Signalling.

Cell-based models. Huh7.5.1 and human stellate LX2 cells were cultured in Dulbecco's Modified Eagle Medium (DMEM) supplemented with 10% heat-decomplemented fetal bovine serum FBS, gentamycin (0.05 mg/mL) and non-essential amino acids (complete DMEM) at 37°C with 5% CO2. For proliferation arrest and differentiation (Huh7.5.1^{dif} cells), Huh7.5.1 cells were cultured in complete DMEM supplemented 1% DMSO[5]. All cell lines were certified mycoplasma-free. To analyze the PLS induction Huh7.5.1^{dif} cells were infected with HCV Jc1 (genotype 2a/2a) as described[6] for a total of 10 days. Cells were then treated with C646 (7.5 µM), CTK7A (1 µM), I-BET151 (50 nM), JQ1 (50 nM), SAHA (0.3 µM), TSA (100 nM), TMP150 (100 nM), WDR5-0103 (25 µM) and MM-102 (25 µM) or BAPTA (3 µM) for 72 h or with Thapsigargin (1 µM) for 24 h. For the FFA model, Huh7.5.1^{dif} cells were co-cultured with 20% LX-2 cells[7]. Following co-culture for 3 days in DMEM supplemented with 10% heat-decomplemented FBS, gentamycin and 1% DMSO at 37°C and 5% CO2, cells were incubated with FFA (800 µM oleic acid and 400 µM palmitic acid) for 72 h, as described[7].

Expression of HCV proteins. The plasmids pEF-JFH1/core191 (expressing the HCV strain JFH1 core cDNA), pEF-JFH1/CE2 (JFH1 core/E1/E2 cDNA), pEF-JFH1/NS5B (JFH1

nonstructural proteins NS3 to NS5B cDNA) were a gift from Dr. Takaji Wakita (Dept. of Virology, National Institute of Infectious Diseases, Tokyo, Japan). To express the different HCV proteins, Huh7.5.1^{dif} cells were transfected with 1 µg of expression plasmids using JetPrimeTM (Polyplus Transfection, VWR International GmbH, Dietikon, Switzerland) according to the manufacturer's instructions. The PLS was assessed 3 days post-transfection.

CRISPR/Cas9 gene editing. The single-guide RNA control (sgCTRL) targeting GFP or sgRNA targeting p300, BRD3, BRD4 and HDAC9 genes were cloned into the lentiGuide-Puro plasmid (Addgene plasmid: #52963). Lentiviruses expressing sgRNA were produced in HEK 293T cells by co-transfection the expression plasmids with an envelope plasmid (pMD2.G) and a packaging plasmid (psPAX2). Co-transfections were performed using the CalPhos™ Mammalian Transfection Kit (Clontech Laboratories) according to manufacturer's instructions. Huh7.5.1 stably expressing Cas-9 endonuclease (Huh7.5.1-Cas9) were generated by transduction of a lentiviral vector expressing Cas9 (pXPR_BRD111, Broad Institute). For knock-out studies, Huh7.5.1-Cas9 cells were infected with lentiviruses expressing the sgRNAs for 48 h. Transduced cells were selected under puromycin treatment (4 µg/mL). The KO efficacy was assessed by Western blot analysis.

Analyses of protein expression. The expression of BRD3, BRD4, c-Myc, HCV core, YAP, phospho-YAP (Ser127) and Actin proteins was assessed by Western blot as described[8], using the Biorad electrophoresis and transfer system. Contrasts of western blotting images were equally adjusted for entire membranes using Bio-Rad image analysis software. Protein expression was assessed using Image Lab software (Biorad) and normalised to total protein amount (Stain-free technology, Biorad).

Jühling F, *et al. Gut* 2020;0:1–13. doi: 10.1136/gutjnl-2019-318918

ChIP-qPCR-assay. The protocol was adapted from[9] with few minor modifications. Liver tissues were dissected from control, DEN-treated or DEN and JQ1 co-treated mice, cut into small pieces and washed in ice cold PBS. Formaldehyde was added [1% final concentration (v/v)] to the PBS containing tissues and incubated on a flip-flop rocker for 10 min at room temperature, followed by addition of 2 M glycine (0.125 M final concentration) and incubation for 5 min (room temperature). Tissues were pelleted (400 g, 5 min) at 4 °C, washed twice in ice-cold PBS and resuspended in 400 µl ice-cold lysis buffer [50 mM Tris-HCl, pH 8.1, 1% (w/v) SDS, 10 mM EDTA, 1X protease inhibitor cocktail (Roche)]. Cross-linked cell-lysates were sonicated at 4°C to generate 200-500 base pair chromatin fragments (Covaris). Cellular debris was removed by spinning (10000 g, 10 min) at 4°C and the supernatant was pre-cleared by incubating with 60 µl protein A/G-agarose beads (pre-blocked with salmon sperm DNA and BSA) for 40 min at 4 °C over a flip-flop rocker. Beads were pelleted (100 g, 1 min) at 4 °C and discarded. Equal amounts of lysates were used for immunoprecipitation. Ten percent of the lysate amount used for immunoprecipitation reaction was saved to be used as input DNA in PCR amplification. Individual samples were diluted 1:8 (v/v) in ChIP dilution buffer [16.7 mM Tris-HCl, pH 8.1, 0.01% (w/v) SDS, 1.1% (v/v) Triton X-100, 1.2 mM EDTA, 16.7 mM NaCl, 1X protease inhibitor cocktail] and incubated overnight with either IgG or anti-BRD4 antibody at 4°C on a flip-flop rocker, followed by incubation with 60 µl protein A/G-agarose beads (pre blocked with salmon sperm DNA and BSA) for 90 min. Immuno-absorbed complexes were recovered by centrifugation (100 g, 1 min) at 4°C. Protein A/G beads were then washed once in low salt buffer [20mM Tris-HCl, pH 8.1, 0.1% (w/v) SDS, 1% (v/v) triton X 100, 2mM EDTA, 150mM NaCl], once in high salt buffer [20mM Tris-HCl, pH 8.1, 0.1% (w/v) SDS, 1% (v/v) triton X 100, 2mM EDTA, 500mM NaCl], once in LiCl buffer [10mM Tris-HCl, pH 8.1, 250mM LiCl, 1% (v/v) NP-40, 1% (w/v) sodium deoxycholate, 1mM EDTA], and finally washed twice in 1ml TE buffer (10mM Tris-HCl, pH 8.0, 1mM EDTA). Chromatin was

released from the beads by incubation with 150 µl elution buffer [1% (w/v) SDS, 100mM NaHCO3] for 15 min at room temperature with intermittent vortexing. The elution step was repeated and both eluates were pooled. One microliter of 10 mg/ml RNase and 5M NaCl (200 mM final concentration) was added to the eluate and incubated at 65°C overnight. Three microliters of 10 mg/ml Proteinase K was then added to the samples and incubated at 50°C for 1 hr. DNA was subsequently purified from the eluate using QIAGEN PCR purification kit (QIAGEN corp.) in a final volume of 50 µl. This purified DNA was next used to perform qPCR using gene-specific primers to reveal BRD4 recruitment in promoter-enhancer regions.

Supplementary references :

1 Kleiner DE, Brunt EM, Van Natta M, *et al.* Design and validation of a histological scoring system for nonalcoholic fatty liver disease. *Hepatol Baltim Md* 2005;**41**:1313–21. doi:10.1002/hep.20701

2 Intraobserver and interobserver variations in liver biopsy interpretation in patients with chronic hepatitis C. The French METAVIR Cooperative Study Group. *Hepatol Baltim Md* 1994;**20**:15–20.

3 Bedossa P, Poynard T. An algorithm for the grading of activity in chronic hepatitis C. The METAVIR Cooperative Study Group. *Hepatol Baltim Md* 1996;**24**:289–93. doi:10.1002/hep.510240201

4 Hoshida Y. Nearest Template Prediction: A Single-Sample-Based Flexible Class Prediction with Confidence Assessment. *PLOS ONE* 2010;**5**:e15543. doi:10.1371/journal.pone.0015543

5 Sainz B, Chisari FV. Production of infectious hepatitis C virus by well-differentiated, growth-arrested human hepatoma-derived cells. *J Virol* 2006;**80**:10253–7. doi:10.1128/JVI.01059-06

6 Pietschmann T, Kaul A, Koutsoudakis G, *et al.* Construction and characterization of infectious intragenotypic and intergenotypic hepatitis C virus chimeras. *Proc Natl Acad Sci U S A* 2006;**103**:7408–13. doi:10.1073/pnas.0504877103

7 Barbero-Becerra VJ, Giraudi PJ, Chávez-Tapia NC, *et al.* The interplay between hepatic stellate cells and hepatocytes in an in vitro model of NASH. *Toxicol Vitro Int J Publ Assoc BIBRA* 2015;**29**:1753–8. doi:10.1016/j.tiv.2015.07.010

8 Krieger SE, Zeisel MB, Davis C, *et al.* Inhibition of hepatitis C virus infection by anti-claudin-1 antibodies is mediated by neutralization of E2-CD81-claudin-1 associations. *Hepatol Baltim Md* 2010;**51**:1144–57. doi:10.1002/hep.23445

9 Mukherji A, Kobiita A, Ye T, *et al.* Homeostasis in intestinal epithelium is orchestrated by the circadian clock and microbiota cues transduced by TLRs. *Cell* 2013;**153**:812–27. doi:10.1016/j.cell.2013.04.020